*Desalination and Water Treatment*
www.deswater.com
doi: 10.5004/dwt.2019.24047

154 (2019) 101–110
June

# Thermodynamic analysis of a heat pump assisted active solar still

Khaoula Hidouri[a,*], M. Mohanraj[b]

[a]*Engineers National School of Gabès, Analysis Processes Unit, Gabès University, Omar Ibn El Khattab Street, 6029 Gabès, Tunisia, email: khaoula2013@yahoo.fr*
[b]*Department of Mechanical Engineering, Hindusthan College of Engineering and Technology, Coimbatore 641032, India, email: mohanrajrac@yahoo.co.in*

Received 17 August 2018; Accepted 1 March 2019

**ABSTRACT**

In this article, the thermodynamic performance of a conventional passive solar still and heat pump assisted active solar still were experimentally investigated and are compared. The experimental observations were made under the climatic conditions of Gabès area in South Tunisia during the months of June and July in the year 2017. The experiments have been carried out in four configurations namely: (a) configuration-I: (0-0-0) (fixed glass cover position (0), single glass cover (0), without heat pump (0)); (b) configuration-II: (1-1-0) (variable glass position (1), double glass cover (1), without heat pump (0)); (c) configuration-III: (0-0-1) (fixed glass position (0), single glass cover (0), with a heat pump (1)) and (d) configuration-IV: (1-1-1) (variable glass position (1), double glass cover (1), with a heat pump (1)). The maximum global energy efficiency of the solar stills has reached to 95%, 90%, 60% and 58% for the configuration-IV: (1-1-1), configuration-III: (0-0-1), configuration-I: (0-0-0) and configuration-II: (1-1-0), respectively. The interior energy was observed to be about 77% for heat pump assisted active solar still configuration-IV (1-1-1) and 48% for the conventional passive solar still configuration-II (1-1-0). The global exergy of a heat pump assisted active solar still configuration-IV (1-1-1) and conventional passive solar still configuration-II (1-1-0) were found to be about 20% and 8%, respectively. Similarly, the internal exergy of heat pump assisted active solar still configuration-IV (1-1-1) and conventional passive solar still configuration-II (1-1-0) was estimated to be about 7.5% and 1.4%, respectively. The heat pump assisted active solar still has improved the yield by about 84.5% when compared with a conventional passive solar still.

*Keywords:* Heat pumps; Solar still; Thermodynamic performance

## 1. Introduction

Water is the key requirement for survival of human beings, animals and other living organisms. The readily available resources from various sources such as sea, rivers and lakes are not possible to drink directly due to the presence of harmful contaminates, bacteria and salt. In addition, the domestic sewage water and industrial effluents needs to be recycled for further use. Desalination is the matured technology to purify the saline water or brackish water or sewage water using conventional energy sources such as coal, natural gas, oils, etc. [1]. The use of these conventional energy resources will create major environmental impacts. Therefore, it is essential to look for energy efficient and environment friendly water purifying technology to meet future demand [2]. Thermal desalination using solar stills is an economical and established technology for purifying water in remote locations facing lack of electricity grid connectivity [3]. However, the productivity of a passive solar still is not enough to meet the demand.

Many research efforts have been made to improve the performance of solar stills, which are summarized in earlier review articles [4–6]. Further improvement in solar still is attained by integrating with a heat pump system. Heat

* Corresponding author.

pumps are the energy efficient heating devices capable of delivering more heat output than work input it takes for compressing the refrigerant [7,8]. Many research initiatives have been progressed on heat pump assisted active solar stills. In a related investigation, Hidouri et al. [9] investigated the performance of a compression heat pump assisted solar still to recover the latent heat of water vapour condensed over the evaporator coils of a heat pump and regenerated to the solar still basin for enhancing the water evaporation. It was reported with improved daily productivity of about 12 L $m^{-2}$, which is about 80% higher than conventional passive solar still. Further, the performance of a heat pump assisted active solar still was enhanced in forced convection mode with an air velocity between 0.04 and 0.08 m $s^{-1}$ [10]. It was reported with improved daily productivity of about 16 L $m^{-2}$. In a similar work, the performance of a heat pump integrated solar still was numerically simulated under the influence of water depth, type of insulation, thickness of insulation and absorption coefficient [11]. It was reported with 75% improvement in productivity when compared with the conventional solar still. The polyurethane with 10 mm thick with 2 cm water depth was identified as a viable insulation to achieve maximum productivity. Other works by Hidouri and Gabsi [12], and Hidouri et al. [13] showed that the energetic performance of a heat pump-assisted active solar distiller is very significant. The performance created the weather conditions of the city Gabès.

Exergy analysis is the power tool for analysing the thermal system to quantify the energy losses. Exergy is an expression used to quantify the energy loss due to entropy generation. The energy loss in the thermodynamic system (exergy destruction) is estimated by multiplying the dead state temperature (ambient temperature) with increase in entropy. Many researchers have used the exergy analysis to quantify the energy losses in the solar stills [14] and also in heat pump systems [15]. In a related work, Torchia-Núñez et al. [16] investigated the exergy performance of a passive solar still and reported that the maximum irreversibility occurred in the basin of the still, which results in poor exergy efficiency. In another work, Asbik et al. [17] investigated the performance of a solar still using paraffin wax heat storage and reported that the exergy efficiency of solar still using paraffin wax heat storage is about 5% during sunshine hours. However, the exergy efficiency was estimated more than 80% during off sunshine hours. Similarly, the thermodynamic performance of a conventional solar still was evaluated with different water depths and reported that highest exergy destruction occurs in the basin of a solar still [18]. They also optimized the water depth to 1 cm based on energy and exergy efficiency. Similarly, the performances of compression heat pump systems were evaluated in terms of exergy destruction and exergy efficiency, which are summarized in earlier review articles [19–21].

The cited literature on thermodynamic analysis of solar stills confirmed that many researchers have tried with energy and exergy analysis of solar stills to quantify the losses in the solar still. However, there is no specific work that has been reported on energy and exergy analysis of heat pump assisted active solar still. Hence, an attempt has been made in this research work to quantify the energy conversion and energy losses in a heat pump assisted active solar still.

## 2. Experiments

The experiments were carried out under the climatic conditions of Tunisia during the months of June and July of the 2017.

### 2.1. Experimental setup

The pictorial diagram of a conventional passive solar still and the heat pump assisted active solar still configuration is depicted in Figs. 1 and 2, respectively. The solar still consists of 0.4 $m^2$ basin made up of 1.2 mm thick mild steel sheet and coated with black paint to improve the absorption rate. The top portion of a solar still was covered with 4 mm thick glass cover and titled with variable glass tilt positions. The glass cover placed over the solar still was maintained with vapour tight using rubber sheets. All the sides of the solar still were adiabatically insulated with 25.4 mm glass wool to reduce the heat loss from the solar still. The water evaporated from the basin gets condensed over the bottom surface of the glass cover and gets collected in a drain channel placed at the bottom surface of a glass cover to collect in the distillate jar. The air–water mixture condensed over the evaporator cooling coils was collected separately in another distillate jar. The solar stills were installed over the stand for experimentation. The depth of water in the basin was maintained constantly at 3 cm in the case of conventional solar still. The water in the basin was heated by means of direct absorption of solar energy harvested through the glass cover. The second solar still configuration consists of a compression heat pump with basic components such as hermetically sealed compressor with rated power input of 200 W, bare tube condenser immersed in the basin of a solar still, capillary tube expansion device and an evaporator to improve the productivity. The water in the basin gets heated by means of direct absorption of solar energy harvested by glass cover and also by means of refrigerant condensation in the heat pump. The evaporator of a heat pump absorbs the latent heat released during condensation of water vapour and regenerated to the basin through the heat pump condenser.

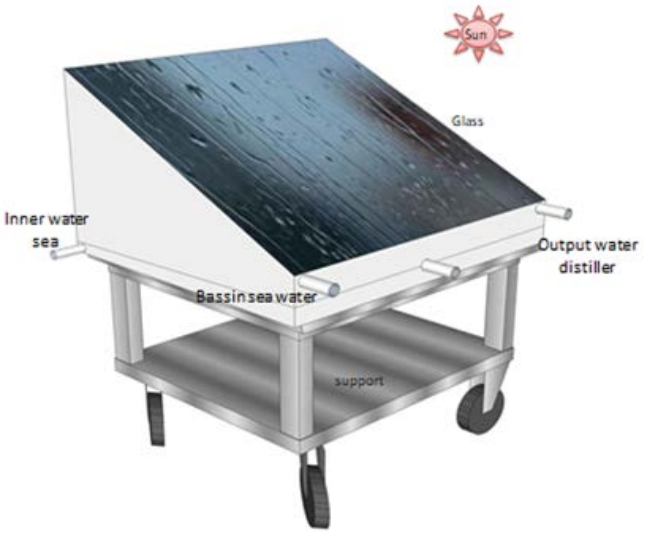


Fig. 1. Pictorial view of conventional solar still.

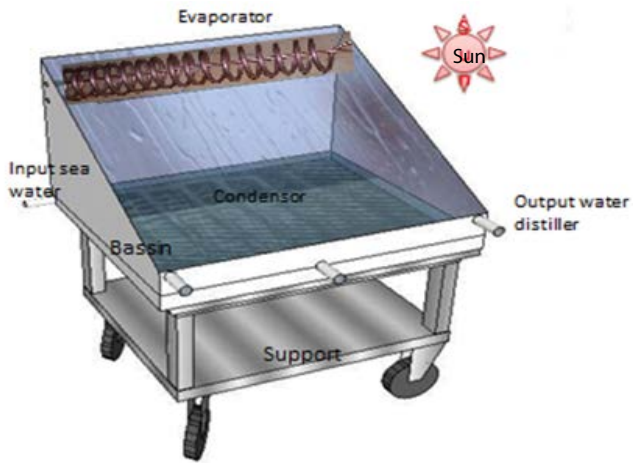


Fig. 2. Pictorial view of heat pump assisted solar still.

### 2.2. Instrumentation

Six k-type calibrated thermocouples with measuring accuracy of ±0.2°C (in the range between 0°C and 100°C) were used for measuring the temperature at different locations in the conventional solar still for measuring the temperature of water in the basin at two different locations, temperature of basin at two different locations, temperature of glass cover and temperature of air–water vapour mixture. Similarly, eight thermocouples were used for measuring the temperature at typical locations as similar to the conventional solar still. In addition, two thermocouples were used for measuring the temperature of an evaporator coil at two locations. All the thermocouples were connected to a digital temperature indicator of 0.1°C resolution and also to a data logger. The ambient temperature was measured using precision thermometer. The solar irradiation was measured using a pyranometer having measuring accuracy of ±5 W $m^{-2}$ (in the range between 0 and 2,000 W $m^{-2}$). The condensate recoveries from the solar stills were collected using calibrated beakers.

### 2.3. Experimental procedure

The experiments were carried out in four different configurations as mentioned in Table 1 during the months of June 2017 and July 2017. The various configurations considered in the experimentation are: (a) fixed glass cover position (represented by 0) and adjustable glass cover position (represented by 1); (b) single (represented by 0) and double glazing cover positions (represented by 1); (c) with heat pump (represented by 0) and without heat pump (represented by 1). The ambient parameters (such as solar irradiation, ambient temperature and ambient wind velocity), solar still operating parameters (such as temperature at different locations in the solar still) and heat pump operating parameters (such as condenser temperature and evaporator temperatures) were measured at 1 h interval from 8.00 h to 18.00 h. Before starting the experimental observations, the basin was filled with required water depth and allowed to attain steady state with ambient conditions to avoid transient errors. Temperatures at the typical locations in both the solar stills, ambient parameters (such as solar irradiation, ambient temperature and ambient wind velocity) and the productivity of both the solar stills were measured every 1 h interval. The condensates (yield or productivity from solar still) were collected in a calibrated beaker separately for the conventional passive solar still and heat pump assisted active solar still. More experimental trials have been made to study the dynamic behaviour of the solar still. The experimental predictions were used for evaluating the energy and exergy performance of a conventional passive solar still and heat pump assisted active solar still.

## 3. Thermodynamic analysis

The thermodynamic equations used for predicting the energy conversion and energy losses of a solar still are presented in this section. The major assumptions made in energy and exergy analysis of a solar still are also listed.

### 3.1. Energy analysis

The energy efficiency a conventional solar still is quantified by using the following equation [9,10]:

$$\eta_{\text{energy}} = \frac{m_w \times L}{A \times I} \tag{1}$$

Here $m_w$ is the mass of water distilled, $A$ is the area of basin (in $m^2$), $I$ is the solar irradiation (in W $m^{-2}$) and $L$ is the latent heat of water vapour (in kJ $kg^{-1}$). The latent heat of water vapour was estimated by the following relation [22]:

$$L = 2.4935 \times 10^6 \times \left(1 - 9.4779 \times 10^{-4} \times T_w + 1.3132 \times 10^{-7} \times T_W^2 - 4.794 \times 10^{-9} \times T_w^3\right) \tag{2}$$

The interior efficiency of simple solar still is given by [9,10]:

Table 1
Study for different configurations

| Fixed position/ variable position | Single glass cover/ double glass cover | Without heat pump/ with heat pump | Configurations |
|---|---|---|---|
| 0 | 0 | 0 | Configuration-I (0-0-0) |
| 1 | 1 | 0 | Configuration-II (1-1-0) |
| 0 | 0 | 1 | Configuration-III (0-0-1) |
| 1 | 1 | 1 | Configuration-IV (1-1-1) |

$$\eta_i = \frac{q_{eww}}{q_w} = \frac{m_w L}{q_w} \tag{3}$$

Here $q_w$ is the quantity of heat absorbed by water.

The global efficiency ($\eta_g$) of a conventional solar still is given by:

$$\eta_g = \frac{q_{ew}}{AI} \tag{4}$$

The interior efficiency of a heat pump assisted active solar still is given by [23]:

$$\eta_i = \frac{q_{ew}}{q_{wc}} \tag{5}$$

Here $q_{wc}$ is the quantity of heat absorbed by water using a heat pump system. It is given by the following relation:

$$q_{wc} = \tau \times AI + q_{cond} = q_w + \alpha_t AI \tag{6}$$

Here $q_{cond}$ is the quantity of heat rejected by a condenser of a heat pump. It is given by the following equation [9,10]:

$$q_{cond} = COP_{PAC} \times W \tag{7}$$

Now, Eq. (5) becomes as follows:

$$\eta_i = \frac{q_{ew}}{\left(\tau \times AI + COP_{PAC} W\right) 3{,}600} \tag{8}$$

Here COP of a heat pump system is given by [9,10]:

$$COP_{PAC} = \frac{q_{cond}}{W} = \frac{T_w}{T_w - T_g} \tag{9}$$

Here $T_w$ and $T_g$ are the water and glass temperatures, respectively.

### 3.2. Exergy analysis

The exergy analysis of a solar still is carried out to quantify the losses in solar stills (conventional and heat pump assisted active solar still). The general exergy balance is given by following equation:

$$\dot{E}x_d = \dot{E}x_{in} - \dot{E}x_{out} \tag{10}$$

The following assumptions are made in exergy analysis [24]:

- All the processes are steady state.
- Vapour leakage from the solar still is assumed to be negligible.
- The effects due to kinetic, potential and chemical are neglected.
- The temperature difference of water in the basin is assumed to be negligible.
- Mechanical and chemical exergy are ignored.
- The properties of solar still given in Table 2 are used for thermal calculations.

#### 3.2.1. Global exergy efficiency

The global exergy efficiency of a conventional passive solar still and heat pump assisted active solar still is given by following equations:

$$\eta_{Ex} = \frac{\sum Ex_{ev}}{\sum Ex_s} \tag{11}$$

Here,

$$Ex_{ev} = \frac{\sum m_w \times L \times \left(\frac{T_a + 273}{T_w + 273}\right)}{3{,}600} \tag{12}$$

The exergy of a solar irradiation that falls on solar still per unit area is given by [25]:

$$Ex_s = A \times I \times \left(1 + 0.33 \times \left(\frac{T_a}{T_s}\right)^4 - 1.33 \times \left(\frac{T_a}{T_s}\right)\right) \tag{13}$$

Here, the sky temperature is estimated using the following relation:

$$T_{sky} = 0.0552 \times T_a^{1/5} \tag{14}$$

#### 3.2.2. Exergy of water

Exergy of water can be obtained by Bejan et al. [26]:

$$Ex_w = m_w \left(c_{pw}\left(T - T_a\right) - T_a R_v \ln\left(\frac{p}{p_0}\right) - T_a c_{pw} \ln\left(\frac{T}{T_a}\right) - R_v T_a \ln\left(\phi_0\right)\right) \tag{15}$$

Table 2
Properties of solar still materials

| Parameter | Value |
|---|---|
| Mass of glass $m_g$, kg m$^{-2}$ | 10.12 |
| Mass of water $m_w$, kg m$^{-2}$ | 20.6 |
| Mass of basin $m_b$, kg m$^{-2}$ | 15.6 |
| Calorific heat capacity of glass $c_{pg}$, J kg$^{-1}$°C | 800 |
| Calorific heat capacity of water $c_{pw}$, J kg$^{-1}$°C | 4,178 |
| Calorific heat capacity of basin $c_{pb}$, J kg$^{-1}$°C | 480 |
| Glass cover absorbability $\alpha_g$ | 0.075 |
| Water absorbability $\alpha_w$ | 0.05 |
| Basin absorbability $\alpha_b$ | 0.95 |
| Glass emissivity $\varepsilon_g$ | 0.88 |
| Water emissivity $\varepsilon_w$ | 0.95 |
| Basin emissivity $\varepsilon_b$ | 0 |
| Glass reflectivity $\rho_g$ | 0.0735 |
| Water reflectivity $\rho_w$ | 0 |
| Basin reflectivity $\rho_b$ | 0 |
| Thermal conductivity of basin $k_b$, W m$^{-1}$°K$^{-1}$ | 16.30 |
| Thermal conductivity of losses $k_l$, W m$^{-1}$°K$^{-1}$ | 0.039 |

The mechanical exergy of water is usually neglected to compare with chemical exergy (because $p_0 = p$ during humidification processes inside the solar still). Hence, the exergy of water becomes:

$$\mathrm{Ex}_w = m_w\left(c_{\mathrm{pw}}\left(T-T_a\right)-T_a c_{\mathrm{pw}}\ln\left(\frac{T}{T_a}\right)-R_v T_a\ln\left(\phi_0\right)\right) \tag{16}$$

*3.2.3. Exergy of humid air*

The total exergy of air during humidification inside the solar still without the influence of kinetic and potential energy is given by following equation [26]:

$$\mathrm{Ex}_a = m_a\left(\begin{array}{l} C_{\mathrm{pa}}+\omega c_{\mathrm{pv}}\left(T-T_a-T_a c_{\mathrm{pw}}\ln\left(\frac{T}{T_a}\right)\right)+ \\ R_a T_a\left(1+1.608\omega\ln\left(\left(\frac{1+1.608\omega_0}{1+1.608\omega}\right)+1.608\omega\ln\left(\frac{\omega}{\omega_0}\right)\right)\right)\end{array}\right) \tag{17}$$

*3.2.4. Interior and external exergy efficiency*

The interior and external exergy efficiencies of a conventional passive solar still and heat pump assisted active solar still configurations are given by the following equations:

$$\eta_{E,\mathrm{PSS}} = \frac{\mathrm{Ex}_{\mathrm{evap}}}{m_w\left(\left(T-T_a\right)-T_a c_{\mathrm{pw}}\ln\left(\frac{T}{T_a}\right)-R_v T_a\ln\left(\phi_0\right)\right)} \tag{18}$$

$$\eta_{E,\mathrm{HPAS}} = \frac{\mathrm{Ex}_{\mathrm{evap}}}{m_w\left(\left(T-T_a\right)-T_a c_{\mathrm{pw}}\ln\left(\frac{T}{T_a}\right)-R_v T_a\ln\left(\phi_0\right)\right)+3{,}600\times\mathrm{COP}_{\mathrm{PAC}}} \tag{19}$$

Here

$$\mathrm{Ex}_{\mathrm{evap}} = Q_{\mathrm{ew}}\left(1-\frac{T}{T_w}\right) \tag{20}$$

*3.2.5. Entropy*

Another important property of interest in the study of the humid air is the entropy of the mixture. The moist air inside the solar still consists of air–vapour mixtures. The specific heat of the air is considered constant and the enthalpy of the water vapour depends on the temperature. The total pressure exerted by the gas mixture is the sum of partial pressure of the components. It is given by the following relation:

$$p = p_a + p_v \tag{21}$$

The dry air moves by convection and the water vapour will move due to evaporation of water from the free surface of the saline water to the inner surface of the glass cover, where it condenses. Thus, moist air contains a quantity of water vapour which can be expressed as [28]:

$$\varphi = \frac{p_a}{p_{\mathrm{sat}}} = \frac{p_a}{\exp\left(25.317-\frac{5{,}144}{Tw+273}\right)} \tag{22}$$

$$\omega = \frac{m_a}{m_v} \tag{23}$$

The relative humidity of air is the function of partial pressures of air. It is given by the following equation [27]:

$$\omega = 0.622\times\left(\frac{p_v}{p_a}\right) = 0.622\times\left(\frac{p_v}{p-p_v}\right) \tag{24}$$

The entropy rate $s_{\mathrm{ha}}$ of the humid air (dry air $s_a$ + water vapour $s_v$), that exists above the saline water surface, per unit time and unit area of the basin, is given by [28]:

$$s_{\mathrm{ha}} = s_a + s_v \tag{25}$$

$$m_{\mathrm{ha}} s_{\mathrm{ha}} = m_a s_a + m_v s_v \tag{26}$$

The corresponding specific entropy rate of the mixture, which is defined as the entropy rate of the mixture per unit mass of dry air, is given by:

$$s_{\mathrm{ha}} = s_a + \omega s_v \tag{27}$$

For a mixture with a humidity ratio w that changes from a reference state ($T_0$ = 0°C, $p_0$ = 611.3 Pa), to a state whose temperature and pressure are $T$ and $p$, the specific entropy of the dry air and the water vapour is, respectively, given by [29,30]:

$$s_a = c_{\mathrm{pa}}\ln\left(\frac{T}{T_a}\right)-R_a\ln\frac{p_a}{p_a}+s_{a0} \tag{28}$$

$$s_v = c_{\mathrm{pv}}\ln\left(\frac{T}{T_a}\right)-R_v\ln\frac{p_v}{p_a}+s_{v0} \tag{29}$$

The entropy of the humid air is given by [28]:

$$s_{\mathrm{ha}} = m_a\left(\ln\left(\frac{T}{T_a}\right)-R_a\ln\left(\frac{p_a}{p_a}\right)\right)+m_v\left(c_{\mathrm{pv}}\ln\left(\frac{T}{T_a}\right)-R_v\ln\left(\frac{p_v}{p_a}\right)\right)+ m_a s_{a0}+m_v s_{v0} \tag{30}$$

## 4. Results and discussion

The experimental observations, energy and exergy performance of a conventional passive solar still and heat pump assisted active solar still operating with four different configurations are measured in this section. In addition, the productivity of a solar still is measured.

The solar flux is the major parameter influencing the performance of solar stills. The solar flux variations observed

during experimentation in solar stills with and without heat pump are depicted in Fig. 3. The observations were made from 8.00 to 18.00 h. It is observed that the solar flux was varied in the range between 150 and 900 W $m^{-2}$. The maximum solar flux was observed during peak sunshine hours. The difference in variation between the experiments was observed to be within 50 W $m^{-2}$. The sunshine duration during experimentation was observed to be in the range between 9 and 12 h. However, the useful solar flux (more than 200 W $m^{-2}$) more than for conversion in solar still is about 8–9 h only. The ambient temperature variations observed during experiments are illustrated in Fig. 4. The maximum ambient temperature of about 34°C was recorded in the time interval between 13.00 and 14.00 h. During early morning and late evening hours, the average ambient temperature was recorded to about 28°C. In addition, the ambient wind velocity variations during experimentations were observed to be about 0.5–3 m $s^{-1}$.

The interior energy efficiency variations observed during experimentation are depicted in Fig. 5. It is observed that the interior energy efficiencies were varied in the range from 42% to 78% for the active solar still configurations-III and IV (0-0-1 and 1-1-1). The maximum energy efficiency of about 78% was observed during peak sunshine hours. But, the energy efficiency variations for the passive conventional solar

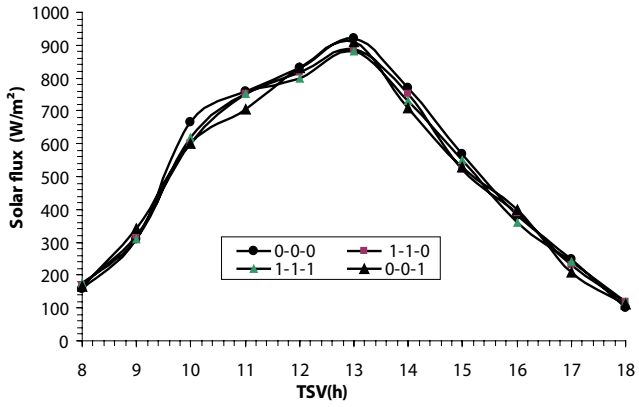


Fig. 3. Variations of solar flux during experimentation of solar stills with and without heat pump.

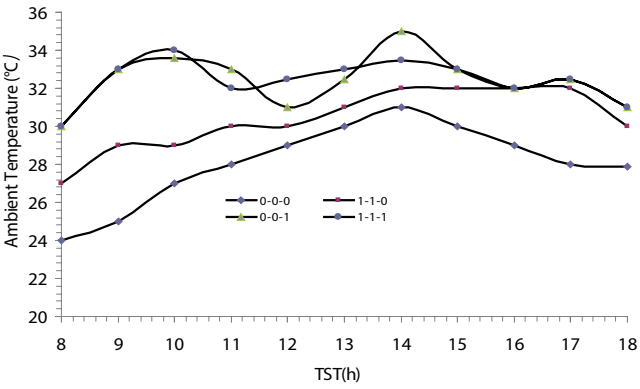


Fig. 4. Variations of ambient temperature during experimentation with and without heat pump.

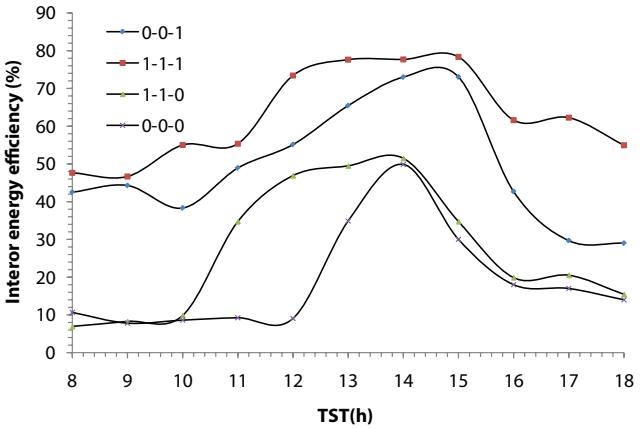


Fig. 5. Variations of interior energy efficiency of solar stills with and without heat pump.

stills varied from about 8% to 48% (for the configurations-I and II, (0-0-0) and (1-1-0)). The maximum interior energy efficiency of about 48% was observed during peak sunshine hours. It is also confirmed that the solar still configuration-IV (1-1-1) with variable glass cover inclination and double glazing has produced higher yield when compared with the fixed position single glazing solar still configuration-III (0-0-1).

Further, the global energy efficiency variations of solar stills with and without heat pump are illustrated in Fig. 6. The global energy efficiency variations are observed to be in the range from about 45% to about 93% in the case of heat pump active assisted solar still configuration-IV (1-1-1) and configuration-III (0-0-1). Similarly, the global energy efficiency of the passive solar still configuration-I (0-0-0) and configuration-II (1-1-0) varied in the range between 10% and 60%. The maximum global energy efficiencies about 92% and 60% were observed during peak sunshine hours for the heat pump assisted active solar stills configurations (such as (1-1-1) and (0-0-1)) and the conventional passive solar still ((0-0-0) and (1-1-0)), respectively. The global energy efficiency of a heat pump assisted active solar still observed in this work is similar to the earlier investigations [9,13] for the heat pump assisted active solar stills.

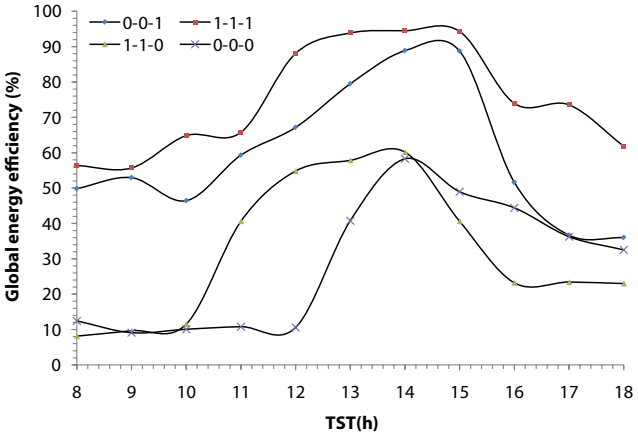


Fig. 6. Variations of global energy efficieny of solar stills with and without heat pump.

The interior exergy efficiency and global exergy variations observed during experimentations with different configurations are compared in Figs. 7 and 8, respectively. From Fig. 7, it is observed that, the passive solar still configuration-I (0-0-0) and configuration-II (1-1-0) have interior exergy variations in the range between 1% and 2%. The heat pump assisted active solar stills have the internal exergy efficiency in the range between 2% and 7.5% for configuration-IV (1-1-1) and between 2% and 6% for configuration-III (0-0-1). The variable glass cover positions have higher internal exergy efficiency when compared with fixed glass cover position. Moreover, it is observed that the double glass cover has influence the interior exergy efficiency of a solar still. From Fig. 8, it is observed that, the global exergy efficiency higher than that of the interior exergy efficiency. The passive configurations ((0-0-0) and (1-1-0)) have global exergy efficiencies of about 10% and for the passive solar still configurations ((0-0-1) and (1-1-1)) have global exergy efficiency of about 17%.

The entropy variations for different solar still configurations are compared in Fig. 9. An increase in pressure of water vapour has enhanced the fast diffusion to the inner glass surface and fast evaporation of water vapour. It is observed that the entropy values get increased in the case of heat pump assisted active solar still when compared with the conventional passive solar still. The entropy of conventional passive solar still configuration-I (0-0-0) and configuration-II (1-1-0) are 3 and 5 J $kg^{-1}$ $K^{-1}$, respectively. The entropy of heat pump assisted active solar still configuration-III and configuration-IV (1-1-1) has reached the maximum value of 12 and 15 J $kg^{-1}$ $K^{-1}$, respectively.

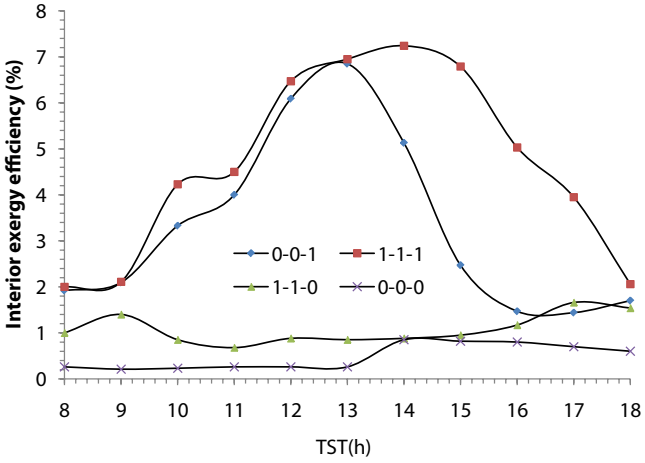


Fig. 7. Variations of interior exergy efficiency of solar stills with and without heat pump.

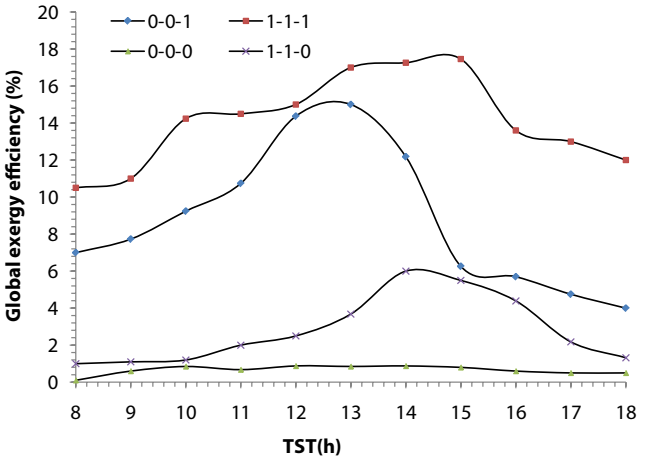


Fig. 8. Variations of global exergy efficiency of solar stills with and without heat pump.

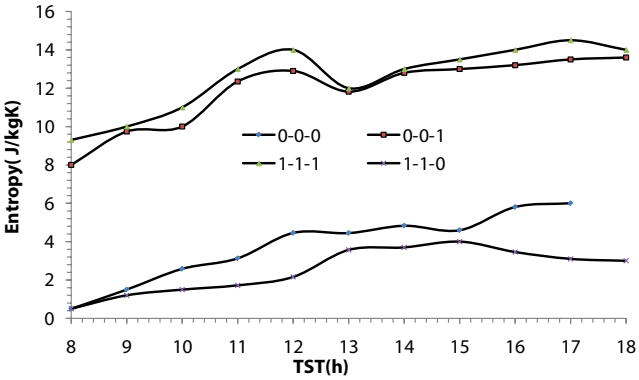


Fig. 9. Variations of entropy of solar stills with and without heat pump.

The hourly productivity of heat pump assisted active solar stills and conventional passive solar stills are compared in Fig. 10. It is observed that the maximum hourly productivity of about 1.75 L of water $m^2$ $h^{-1}$ was obtained in the case of heat pump assisted active solar still configuration-IV (1-1-1) followed by heat pump assisted solar still with the productivity of 1.4 L of water per $m^2$ $h^{-1}$ for heat pump assisted active solar still configuration-III (0-0-1). The conventional passive solar still configurations-I and II are having lower hourly yield in the range of 0.4 L of water $m^{-2}$ $h^{-1}$. The hourly yield of solar still was found to be similar to the earlier reported investigations [9,10,13].

From Fig. 11, it is observed that the heat pump assisted active solar stills with configuration-IV (1-1-1) and

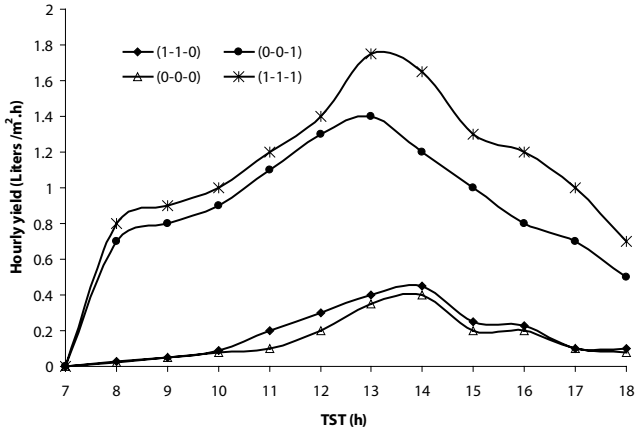


Fig. 10. Hourly yield of solar stills with and without heat pump.

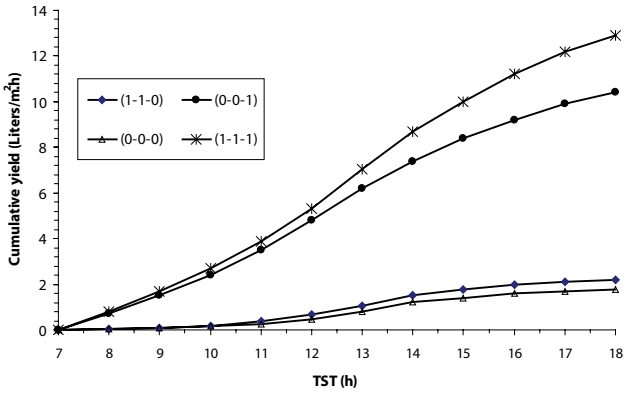


Fig. 11. Cumulative yield of solar stills with and without heat pump.

configuration-III (0-0-1) have produced the cumulative yield of about 12.9 and 10.9 L of water $m^{-2}$ $d^{-1}$, respectively. The conventional passive solar still configurations-I and II have produced the maximum yield of about 2 L of water $m^{-2}$ $d^{-1}$ only. The experimental observations confirmed that the heat pump assisted active solar stills have produced about 84.5% higher yield when compared with the conventional solar stills. The improvement in yield obtained in this work is similar to the earlier research investigations reported by Hidouri et al. [31,32].

## 5. Conclusion

The thermodynamic analysis of a conventional passive solar still and heat pump assisted active solar still was investigated experimentally under the climatic conditions of Tunisa during the months of June and July in the year 2017. The following major conclusions are drawn:

- The interior energy was estimated to be about 78% for a heat pump asissted active solar still configuration-IV (1-1-1) and 48% for the conventional passive solar still configuration-I (0-0-0).
- The maximum global energy efficiency of a heat pump assisted active solar still configuration-IV (1-1-1) has reached more than 90% during peak sunshine hours. Whereas, the conventional passive solar still confiugration-I (0-0-0) has attained the maximum global energy efficiency of about 50%. About 40% improvement in energy efficiency was observed with heat pump assisted active solar still configuration-IV (1-1-1) when comparted with conventional passive solar still configuraiton-I (0-0-0).
- The maximum global exergy of a heat pump assisted active solar still configuration-IV (1-1-1) and simple passive solar still configuration-I were found to be about 20% and 8%, respectively.
- Similarly, the interior exergy of a heat pump assisted active solar still confiugration-IV (1-1-1) and conventional solar still configuration-I (0-0-0) was estimated to be about 7.5% and 1.4%, respectively.
- The productivity of a heat pump assisted active solar still configuration-IV (1-1-1) was found to be about 84.5% higher when compared with the covnentional passive solar still configuration-I (0-0-0).

The results confirmed that the heat pump assisted active solar still configuratiuon-IV with variable glass cover positions and double glass cover (1-1-1) has achieved the maximum thermodynmaic performance and produced maximum productivity when compared with other configurations investigated.

## Symbols

$A$ — Basin area, $m^2$
$c_{pa}$ — Specific heat of dry air, J $kg^{-1}$ $K^{-1}$
$c_{pv}$ — Specific heat of water vapour, J $kg^{-1}K^{-1}$
$COP_{PAC}$ — Coefficient of performance
$c_{pw}$ — Specific heat of water, J $kg^{-1}K^{-1}$
$c_{pg}$ — Specific heat of glass, J $kg^{-1}K^{-1}$
$c_{pb}$ — Specific heat of basin, J $kg^{-1}K^{-1}$
$E_{xa}$ — Exergy of humid air, W $m^{-2}$
$E_d$ — Exergy destruction, W $m^{-2}$
$E_{xev}$ — Exergy output of solar still, W $m^{-2}$
$E_{xs}$ — Exergy of solar irradiation, W $m^{-2}$
$E_{xw}$ — Exergy of water, W $m^{-2}$
$q_w$ — Heat quantity absorbed by water, W $m^{-2}$°C
$q_{wc}$ — Heat quantity absorbed by water in the use of heat pump, W $m^{-2}$
$q_{cond}$ — Heat condenser water, W $m^{-2}$
$q_{ew}$ — Heat flux water use for the evaporisation, W $m^{-2}$
$k_b$ — Thermal conductivity of basin, W $m^{-1}$°C
$k_\lambda$ — Thermal conductivity of losses, W $m^{-1}$°C
$I$ — Solar irradiation, W $m^{-2}$
$P$ — Total pressure of humid air, Pa
$P_a$ — Partial pressure of dry air, Pa
$P_v$ — Partial pressure of water vapour, Pa
$P_0$ — Saturated water vapour pressure, Pa
$L$ — Latent heat of water vapour, in terms of kJ $kg^{-1}$
$m_w$ — Mass flow rate of water vapour, kg $h^{-1}$ $m^{-2}$
$m_a$ — Mass flow rate of saturated water vapour, kg $h^{-1}$ $m^{-2}$
$m_g$ — Mass of glass, kg $m^{-2}$
$m_b$ — Mass of basin, kg $m^{-2}$
$S$ — Entropy, J $K^{-1}$
$S_a$ — Entropy rate of dry air per unit area of basin, W $m^{-2}$ $K^{-1}$
$S_{ha}$ — Entropy rate of humid air per unit area of basin, W $m^{-2}$ $K^{-1}$
$S_0$ — Entropy rate of water vapour per unit area of basin, W $m^{-2}$ $K^{-1}$
$s$ — Specific entropy, J $kg^{-1}$ $K^{-1}$
$s_{a0}$ — Specific entropy of the saturated air vapour at reference conditions, J $kg^{-1}$ $K^{-1}$
$s_{v0}$ — Specific entropy of the saturated water vapour at reference conditions, J $kg^{-1}$ $K^{-1}$
$R$ — Universal gas constant of ideal gases, J $mol^{-1}$ $K^{-1}$
$R_a$ — Gas constant of dry air, J $kg^{-1}$ $K^{-1}$
$R_v$ — Gas constant of water vapour, J $kg^{-1}$ $K^{-1}$
$T_w$ — Water temperature, K
$T_g$ — Glass temperature, K
$T_a$ — Ambient temperature, K
$T_s$ — Sun temperature, K
$W$ — Compressor power, Watt

**Greek letters**

$\alpha_g$ — Glass cover absorbability
$\alpha_w$ — Water absorbability
$\alpha_b$ — Basin absorbability
$\rho_g$ — Glass reflectivity
$\rho_w$ — Water reflectivity
$\rho_b$ — Basin reflectivity
$\varepsilon_g$ — Glass emissivity
$\varepsilon_w$ — Water emissivity
$\varepsilon_b$ — Basin emissivity
$\eta_{energy}$ — Energy efficiency
$\eta_I$ — Interior energy efficiency
$\eta_g$ — Global energy efficiency
$\eta E_x$ — Global exergy efficiency
$\eta E_{PSS}$ — Interior exergy efficiency for conventional solar still
$\eta E_{HPAS}$ — Interior exergy efficiency for hybrid solar still
$j$ — Relative humidity, %
$w$ — Humidity rate, %

**References**


[1] D. Xevgenos, K. Moustakas, D. Malamis, M. Loizidou, An overview on desalination & sustainability: renewable energy-driven desalination and brine management, Desal. Wat. Treat., 57 (2016) 1–11.
[2] T. Arunkumar, K. Raj, D.D.W. Rufuss, D. Denkenberger, G. Tingting, L. Xuan, R. Velraj, A review of efficient high productivity solar stills, Renewable Sustainable Energy Rev., 101 (2019) 197–220.
[3] F.E. Ahmed, R. Hashaikeh, N. Hilal, Solar powered desalination – Technology, energy and future outlook, Desalination, 453 (2019) 54–76.
[4] R. Balan, J. Chandrasekaran, S. Shanmugan, B. Janarthanan, S. Kumar, Review on passive solar distillation, Desal. Wat. Treat., 28 (2011) 217–238.
[5] M. Chandrashekara, A. Yadav, Water desalination system using solar heat: a review, Renewable Sustainable Energy Rev., 67 (2017) 1308–1330.
[6] A. Kaushal, Varun, Solar stills: a review, Renewable Sustainable Energy Rev., 14 (2010) 446–453.
[7] M.N.A. Hawlader, P.K. Dey, S. Diab, C.Y. Chung, Solar assisted heat pump desalination system, Desalination, 168 (2003) 49–54.
[8] M. Mohanraj, Y. Belyayev, S. Jayaraj, A. Kaltayev, Research and developments on solar assisted compression heat pump systems – a comprehensive review (Part-B: Applications), Renewable Sustainable Energy Rev., 83 (2018) 124–155.
[9] K. Hidouri, R. Ben Slama, S. Gabsi, Hybrid solar still by heat pump compression, Desalination, 250 (2010) 444–449.
[10] K. Hidouri, A. Benhmidene, M.E.H. Assad, B. Chaouachi, Experimental evaluation of the effect of air velocity in hybrid solar distiller, Desal. Wat. Treat., 107 (2018) 20–27.
[11] H. Ben Halima, N. Frikha, R. Ben Slama, Numerical investigation of a simple solar still coupled to a compression heat pump, Desalination, 337 (2014) 60–66.
[12] K. Hidouri, S. Gabsi, Correlation for Lewis number for evaluation of mass flow rate for simple/hybrid solar still, Desal. Wat. Treat., 57 (2016) 6209–6216.
[13] K. Hidouri, B. Ali, B.S. Rhomdanne, G. Slimane, Effects of SSD and SSDHP on convective heat transfer coefficient and yields, Desalination, 249 (2009) 1259–1264.
[14] P. Dumka, D.R. Mishra, Energy and exergy analysis of conventional and modified solar still integrated with sand bed earth: study of heat and mass transfer, Desalination, 437 (2018) 15–25.
[15] M. Mohanraj, S. Jayaraj, C. Muraleedharan, Exergy analysis of direct expansion solar-assisted heat pumps using artificial neural networks, Int. J. Energy Res., 33 (2009) 1005–1020.
[16] J.C. Torchia-Núñez, M.A. Porta-Gándara, J.G. Cervantes-de Gortari, Exergy analysis of a passive solar still, Renewable Energy, 33 (2008) 608–616.
[17] M. Asbik, O. Ansari, A. Bah, N. Zari, A. Mimet, H. El-Ghetany, Exergy analysis of solar desalination still combined with heat storage system using phase change material (PCM), Desalination, 381 (2016) 26–37.
[18] S. Vaithilingam, G.S. Esakkimuthu, Energy and exergy analysis of single slope passive solar still: an experimental investigation, Desal. Wat. Treat., 55 (2015) 1433–1444.
[19] M. Mohanraj, Ye. Belyayev, S. Jayaraj, A. Kaltayev, Research and developments on solar assisted compression heat pump systems – A comprehensive review (Part A: Modeling and modifications), Renewable Sustainable Energy Rev., 83 (2018) 90–123.
[20] J.U. Ahamed, R. Saidur, H.H. Masjuki, A review on exergy analysis of vapor compression refrigeration system, Renewable Sustainable Energy Rev., 15 (2011) 1593–1600.
[21] O. Ozgener, A. Hepbasli, A review on the energy and exergy analysis of solar assisted heat pump systems, Renewable Sustainable Energy Rev., 11 (2007) 482–496.
[22] C. Elango, N. Gunasekar, K. Sampathkumar, Thermal models of solar still—A comprehensive review, Renewable Sustainable Energy Rev., 47 (2015) 856–911.
[23] J.A. Clark, The steady-state performance of a solar still, Sol. Energy, 44 (1990) 43–49.
[24] Y.A. Cengel, M.A. Boles, Thermodynamics: An Engineering Approach, 7th Ed., McGraw-Hill, New York, 2010.
[25] R. Petela, Exergy of undiluted thermal radiation, Sol. Energy, 74 (2003) 469–488.
[26] A. Bejan, D.W. Kearney, F. Kreith, Second law analysis and synthesis of solar collector systems, Sol. Energy, 103 (1981) 23–28.
[27] W.Z. Black, J.G. Hartley, Thermodynamics, Harper and Row, Publishers, Inc., New York, 1985.
[28] K.R. Ranjan, S.C. Kaushik, N.L. Panwar, Energy and exergy analysis of passive solar distillation systems, Int. J. Low-Carbon Technol., 11 (2016) 211–221.
[29] S. Yemna, H. Nejib, M. Ali, B.B. Ammar, Study of heat and mass transfer phenomena and entropy rate of humid air inside a passive solar still, Desalination, 409 (2017) 80–95.
[30] O. Bait, M. Si–Ameur, Numerical investigation of a multi-stage solar still under Batna climatic conditions: effect of radiation term on mass and heat energy balances, Energy, 98 (2016) 308–323.
[31] K. Hidouri, R. Mishra, Dhananjay, Experimental Evaluation of influence of air injection rate on a novel single slope solar still integrated with an air compressor, Global J. Res. Eng. A Mech. Mech. Eng., 17 (2017) 30–39.
[32] K. Hidouri, A. Benhmidene, B. Chaouachi, S. Ravishankar, Comparative study for evaluation of mass flow rate for simple solar still and active with heat pump, J. Water Environ. Nanotechnol., 2 (2017) 157–165.

## Appendices

### Appendix A: Physical properties of humid air

| Physical property | Unit | Expression |
|---|---|---|
| Specific heat capacity, $c_{pa}$ | J kg$^{-1}$ K$^{-1}$ | $999.2 + 0.1343T + 1.01 \times 10^{4}T^{2} - 6.758 \times 10^{-8}T^{3}$ |
| Thermal conductivity, λ | W m$^{-1}$ K$^{-1}$ | $1.718 \times 10^{-5} + 4.62 \times 10^{-8}T$ |
| Viscosity, μ | Pa s | $353.44/(T + 273.15)$ |
| Expansion factor | kg m$^{-3}$ | $1/(T + 273.15)$ |
| Saturated vapour pressure | Pa | Exp(25.317–5,144/(273.15 + $T$) |

### Appendix B: Physical constants of dry air and water vapour used in the range of the studied humid air temperature

| Physical property | Unit | Value |
|---|---|---|
| Dry air molecular mass, $m_a$ | kg k$^{-1}$ mol$^{-1}$ | 28.97 |
| Water vapour molecular mass, $m_v$ | kg k$^{-1}$ mol$^{-1}$ | 18 |
| Gas constant of water vapour, $R_v$ | J kg$^{-1}$ K$^{-1}$ | 461.89 |
| Gas constant of air vapour, $R_a$ | J kg$^{-1}$ K$^{-1}$ | 287.1 |
| Dry air of specific heat capacity, $c_{pa}$ | J kg$^{-1}$ K$^{-1}$ | 1,009 |
| Water vapour of specific heat capacity, $c_{pv}$ | J kg$^{-1}$ K$^{-1}$ | 1,820 |
| Reference temperature, $T_0$ | K | 273.15 |
| Reference pressure, $P_0$ | Pa | 611.3 |
| Saturated vapour specific entropy, $s_{v0}$ (at $T_0$ = 273.15 K $P_0$ = 611.3 Pa) | J kg$^{-1}$ K$^{-1}$ | 9,156.2 |